Available online at www.sciencedirect.com
SCIENCE DIRECT®
Journal of Solid State Chemistry 177 (2004) 319–331
JOURNAL OF SOLID STATE CHEMISTRY
http://elsevier.com/locate/jssc

High-temperature transformations of Cu-rich hydrotalcites

S. Kannan,[a,*] V. Rives,[b] and H. Knözinger[c]

[a] *Silicates and Catalysis Discipline, Central Salt and Marine Chemicals Research Institute, Bhavnagar 364 002, India*
[b] *Departamento de Química Inorgánica, Universidad de Salamanca, 37008-Salamanca, Spain*
[c] *Department Chemie, Physikalische Chemie, Universität München, Butenandtstrasse 5–13 (Haus E), 81377 München, Germany*

Received 31 May 2003; received in revised form 12 August 2003; accepted 20 August 2003

Abstract

CuM(II)Al ternary hydrotalcites (M(II) = Ni, Co and Mg) with a (Cu + M(II))/Al atomic ratio of 3.0 and Cu/M(II) atomic ratio of 5.0 were synthesized by coprecipitation under low supersaturation. Powder X-ray diffraction of the as-synthesized samples showed a pattern characteristic of hydrotalcite-like (HT-like) structure (JCPDS: 41-1428). Thermal analyses of these samples showed four stages of weight loss/heat change when recorded in nitrogen. Analysis of the evolved gases characterized the nature of these transformations. The thermoanalytical effects differed significantly especially for the high-temperature transformations, when the treatment was performed in oxygen. In situ powder X-ray diffraction of the samples was carried out to elucidate the phase evolution of these compounds. Surprisingly formation of CuO was noted at temperatures around 200°C well below the destruction of the layered network. The nature of the resulting phases varied with both the nature of the co-bivalent metal ion and the heating atmosphere. FT-IR spectroscopy confirmed the retention of carbonate ions at higher temperatures (above 700°C), although the concentration of carbonate anion (most likely unidentate) varied with the calcination temperature. The crystallinity of CuO increased significantly above 600°C, probably through dissociation of copper oxycarbonate. Significant differences in the thermal transformation temperatures (for the third and the fourth transformations) of these samples containing different co-bivalent metal ions were not observed. This suggests that an association of the co-bivalent metal ions and/or trivalent metal ion in this phase is unlikely. A plausible thermal evolution scheme of these hydrotalcites is proposed.

Keywords: Cu-hydrotalcite; In situ powder X-ray diffraction; Thermal behavior; FT-IR spectroscopy

1. Introduction

Hydrotalcite-like compounds are two-dimensional layered materials with alternating positively charged mixed metal hydroxide sheets and negatively charged interlayer anions along with water molecules [1]. They are represented by the general formula $[M(\mathrm{II})_{1-x}M(\mathrm{III})_x(\mathrm{OH})_2][A^{n-}_{x/n}]\cdot m\mathrm{H_2O}$ where M(II) is a bivalent metal ion, M(III) is a trivalent metal ion, A is the interlayer anion, and x can have values between 0.2 and 0.4 [2]. Transition metal containing hydrotalcites, particularly copper-containing hydrotalcites are receiving increasing attention owing to their diverse catalytic applications [3–7]. Understanding the thermal behavior of these materials is important since they are used as catalysts after calcination [8]. In our earlier work [9], we have observed an endothermic high-temperature effect around 600°C, which is characteristic of copper-containing hydrotalcites, as also reported by others [10,11]. Velu and Swamy [10] have observed this effect for CuMnAl hydrotalcite and attributed this feature to a reaction occurring between brucite sheets and carbonate anions to form an oxycarbonate of chemical composition $M(\mathrm{II})M(\mathrm{III})_xO_y(CO_3)_z$. However, Alejandre et al. [11] have found a similar thermal feature in an attempt to synthesize pure CuAl hydrotalcites and attributed this effect to differences in the coordination of carbonate anions within the brucite-like lattice. Fierro and coworkers [12] reported the thermal decomposition of CuZnAl ternary hydrotalcite having an (Cu + Zn)/Al atomic ratio of 3.0 and Cu/Zn atomic ratio of 0.5. They attributed the high-temperature transformations occurring around 600°C to the removal of carbonate anions occluded in the solid and demonstrated by FT-IR spectroscopy that coordination of carbonate anions in

*Corresponding author. Fax: +91-278-2566970.
E-mail address: kanhemad1@sancharnet.in (S. Kannan).

0022-4596/$ - see front matter © 2003 Elsevier Inc. All rights reserved.
doi:10.1016/j.jssc.2003.08.023

the interlayer space changes upon loss of interlayer water molecules. Although thermal properties of copper-containing hydrotalcites have been investigated in the past, a detailed account of the high-temperature processes, particularly at temperatures greater than 600°C, is still lacking. The aim of this paper is to unravel these high-temperature effects by varying both the co-bivalent metal ions associated with copper and the gas atmosphere. The need for studying various co-bivalent metal ions (both redox as well as non-redox) is to understand their influence on these high-temperature transformations.

2. Experimental

The samples were prepared by coprecipitation under low supersaturation. Two solutions, namely, solution (A) containing the desired amount of metal (Cu, Co, Ni, Mg and Al) nitrates and solution (B) containing the precipitating agents (i.e., NaOH and Na_2CO_3) were added slowly ($\sim 1\,mL\,min^{-1}$) and simultaneously into a beaker containing distilled water, while maintaining the pH constant around 9–10 under vigorous stirring at room temperature. The addition of these solutions took ca. 90 min and the final pH was adjusted to 10. The samples were aged in the mother liquor at 65°C for 18 h, filtered off, washed (until total absence of nitrates in the washing liquids and neutral pH) and dried in an air oven at 110°C for 12 h. In all cases, the atomic ratio between the divalent and trivalent cations was maintained around 3.0, while the Cu:*M*(II) atomic ratio was 5:1. The reason for selecting higher Cu-content in our samples is that the weight loss corresponding to high-temperature transformations (occurring above 600°C) is higher when the Cu-content was higher, assisting in precise analysis of results. The samples are denoted Cu*M*(II)Al-HT where *M*(II) = Ni, Co and Mg. Binary CuAl hydroxycarbonate was also prepared and included in this study for comparison.

3. Techniques

Elemental chemical analysis for Cu, Mg, Co, Ni, and Al was carried out by atomic absorption in a Mark 2 ELL-240 apparatus, in Servicio General de Analisis Quimico Aplicado (University of Salamanca, Spain).

Powder X-ray diffraction (PXRD) patterns were recorded on a Siemens D-500 instrument, using Cu$K\alpha$ radiation ($\lambda = 1.54050$ Å). Data analysis was carried out with AT Diffract software. In situ powder X-ray diffraction (PXRD) was carried out on a Philips X'Pert MPD system connected to an Anton-Paar high-temperature XRK assembly using Cu$K\alpha$ radiation. The sample was mounted in a high-temperature cell and heated at $5°C\,min^{-1}$ in steps of 50°C and stabilized for 5 min before measurements. The operating voltage and current were 40 kV and 40 mA, respectively. The step size was 0.05° with a step time of 1 s. Identification of the crystalline phases was made by comparison with the JCPDS files [13].

FT-IR spectra were recorded on a Perkin-Elmer FT1730 instrument using KBr pellets; 100 spectra (recorded with a nominal resolution of $4\,cm^{-1}$) were averaged to improve the signal-to-noise ratio. In situ FT-IR spectroscopy studies were carried out with a Bruker IFS-66 apparatus at a spectral resolution of $2.0\,cm^{-1}$ accumulating 128 scans. Self-supporting wafers (ca. $10\,mg\,cm^{-2}$) were prepared from the sample and heated directly in a purpose-made IR cell. The latter was connected to a vacuum/sorption apparatus with a residual pressure less than 10^{-3} Pa.

Thermogravimetric (TG) and differential thermal analyses (DTA) were carried out on TG-7 and DTA-7 instruments from Perkin-Elmer in flowing oxygen or nitrogen (from L'Air Liquide, Spain, flow $50\,mL\,min^{-1}$) at a heating rate of $10°C\,min^{-1}$. Alumina (Merck) calcined at 1200°C was used as a reference for the DTA measurements. The gases evolved during thermal treatment were simultaneously analyzed by an on-line quadruple mass spectrometer (Balzers 420) connected with a Netzsch thermo balance with a focus on m/e = 18 (H_2O) and 44 (CO_2).

Specific surface area measurement and pore size analysis was carried out on a Gemini instrument from Micromeritics. The sample (ca. 80–100 mg) was previously degassed in flowing nitrogen at 150°C for 2 h in order to remove physisorbed water in a FlowPrep060 apparatus, also from Micromeritics, and the data were analyzed using published software [14].

4. Results and discussion

Elemental chemical analysis of the samples (Table 1) showed a reasonable correspondence within experimental error limits between the (Cu + *M*(II))/Al and Cu/*M*(II) atomic ratios of the solids and the starting solutions suggesting completion of precipitation. The lack of coincidence between the initial ratio of cations in the solutions and the ratio in the solids isolated, is, however, rather common in literature, and has been ascribed to a preferential precipitation of one or another cation as hydroxide [15]. The molecular formulae of the samples were calculated and are given in Table 1. In deriving the molecular formula, it was assumed that the carbonate is the only charge compensation anion (see also FT-IR data), while interlayer water was calculated from TG curves. Further, TPR and UV-vis analysis of these samples also confirmed the retention of +2

Table 1
Elemental composition and formula of the samples synthesized

Sample	(Cu + *M*(II))/Al[a]		Cu/*M*(II)[a]		Formula[b]
	Solution	Solid	Solution	Solid	
CuMgAl-HT	3.0	3.06	5.0	5.18	$[Cu_{0.63}Mg_{0.12}Al_{0.25}(OH)_2](CO_3)_{0.13}\cdot 0.58H_2O$
CuNiAl-HT	3.0	3.04	5.0	4.40	$[Cu_{0.61}Ni_{0.14}Al_{0.25}(OH)_2](CO_3)_{0.13}\cdot 0.96H_2O$
CuCoAl-HT	3.0	2.96	5.0	4.60	$[Cu_{0.62}Co_{0.13}Al_{0.25}(OH)_2](CO_3)_{0.13}\cdot 0.62H_2O$

[a] Atomic ratio.
[b] Values rounded to two significant figures.

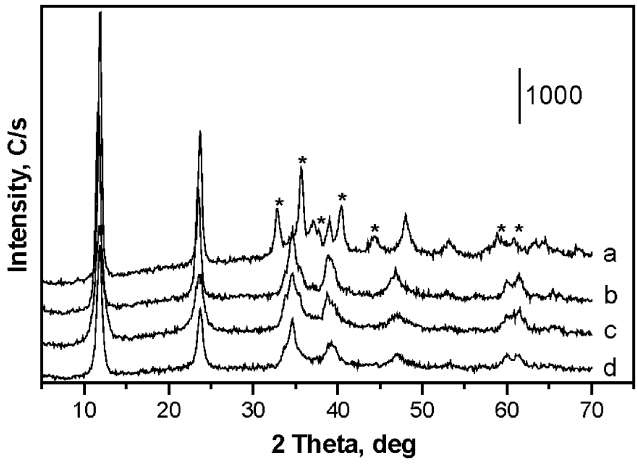

Fig. 1. Powder X-ray diffraction patterns of (a) CuAl-HT, (b) CuMgAl-HT, (c) CuNiAl-HT, (d) CuCoAl-HT (* - gerhardite).

oxidation state for these metal ions in the brucite-like network.

Powder X-ray diffraction patterns of these three samples along with binary CuAl-HT (Cu/Al atomic ratio is 3.0) are shown in Fig. 1. All three ternary hydrotalcites crystallized in HT-like phase without any discrete crystalline impurity, exhibiting sharp and symmetric reflections at lower diffraction angles. On the contrary, binary CuAl-HT consisted of a mixed phase containing both gerhardite (or malachite) and hydrotalcite [11, 16–18]. The lack of single-phase crystallization as HT-like structure of CuAl-HT is well known [1] and accounted for by the Jahn–Teller distortion of copper in octahedral coordination. Among the three bivalent metal ions studied, Mg offered a well-ordered material followed by nickel and cobalt. Lattice parameters '*a*' and '*c*' were calculated from the first peak of the doublet observed near $2\theta = 60°$ (diffraction by (110) planes) and the first basal peak observed near $2\theta = 12°$ (diffraction by (003) plane), respectively. The numerical values are summarized in Table 2. It is seen that the values are very nearly identical, although small variations in '*a*' result from the differences in the ionic radii of the bivalent metal ions [19]. The '*c*' parameter is a measure of the Coulomb forces between layer and interlayer, and their almost identical values suggest a similar extent of electrostatic interaction irrespective of the nature of the cobivalent metal ions. BET measurements showed a maximum specific surface area for CuNiAl-HT and a minimum for CuCoAl-HT, whose values along with pore volumes are also summarized in Table 2.

Table 2
Lattice parameters, surface areas and pore volumes of as-prepared samples

Sample	*a* (Å)	*c* (Å)	S_{BET} ($m^2\,g^{-1}$)	V_p ($cm^3\,g^{-1}$)
CuMgAl-HT	3.081	22.78	60	0.48
CuNiAl-HT	3.074	22.48	89	0.23
CuCoAl-HT	3.081	22.43	32	0.07

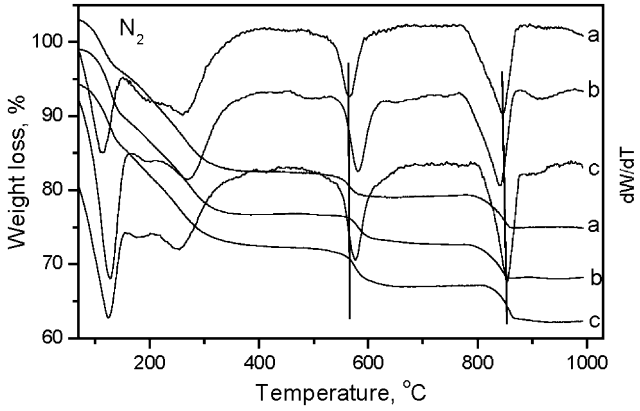

Fig. 2. TG and DTG traces of (a) CuNiAl-HT, (b) CuMgAl-HT, (c) CuCoAl-HT recorded in nitrogen.

Thermogravimetric and differential thermal analyses of these samples were carried out both in nitrogen and in oxygen, in order to detect any oxidation process occurring during calcination. The TG curves together with the corresponding derivative TG curves (DTG) recorded in nitrogen are shown in Fig. 2 and the parameters are summarized in Table 3. The reasons for these transformations are summarized below.

Up to four different stages can be envisaged in the TG curves recorded in nitrogen. According to data

Table 3
Thermogravimetric parameters of the samples synthesized

Sample	T_1 (°C)	T_2 (°C)	T_3 (°C)	T_4 (°C)	W_3 (%)	W_4 (%)	Net weight loss (%)
CuMgAl-HT (N)[a]	127	270	565	846	3.3	4.6	28.1
CuNiAl-HT (N)[a]	114	261	576	852	3.0	4.4	32.0
CuCoAl-HT (N)[a]	126	253	582	840	5.1	4.6	29.9
CuMgAl-HT (O)[b]	129	245[c]	588		4.1		26.2
CuNiAl-HT (O)[b]	114	230[c]	577		3.9		25.3
CuCoAl-HT (O)[b]	124	228[c]	584		4.5		27.4

[a] Heated under nitrogen.
[b] Heated under oxygen.
[c] Center of the broad peak.

previously reported [20], the first weight loss, identified by a rather sharp DTG minimum at 104–121°C corresponds to removal of interlayer water molecules. This weight loss was immediately followed by a second weight loss, up to ca. 350°C. The corresponding DTG signal covers a broad temperature window and splits into two broad overlapping signals, usually attributed to dehydroxylation of the brucite-like layers and decarbonation. Gas evolution analysis (Fig. 3) showed that the first DTG signal is only related to dehydration through removal of the interlayer water molecules (no evolution of CO_2 was noted till 200°C) while the second transformation comprises both dehydroxylation and decarbonation. Generally, for MgAl-hydrotalcites, such a weight loss (due to decarbonation and dehydroxylation) extends up to ca. 500°C, and no further weight loss is usually recorded above this temperature. However, in the case of transition metal containing hydrotalcites, particularly with those containing copper, additional transformations were noted. Two well-defined transformations were noted in the temperature range between ca. 590°C and 850°C. However, their position did not significantly vary with the nature of the bivalent metal ions (Fig. 2). For the third transformation (occurring around 590°C), the variation was around ± 10°C while for the fourth transformation it was only around ± 5°C. These minor variations remain within the temperature resolution of the instrument and/or are related to different textural effects of the solids. We therefore infer that these transformations are only scarcely influenced by the nature of the co-bivalent metal ion. In other words, these transformations seem to be characteristic of copper-containing phases. Further, these transformations occur in a rather narrow temperature range (more clear from DTG traces). This suggests that these transformations should involve structural transformations. A total weight loss of around 30% was observed for these samples, of which the first two weight losses account for $\sim 21\%$ while the latter two weight losses contribute around 9%. The net weight loss of the two high-temperature transformations (third and fourth put together) was very similar for these

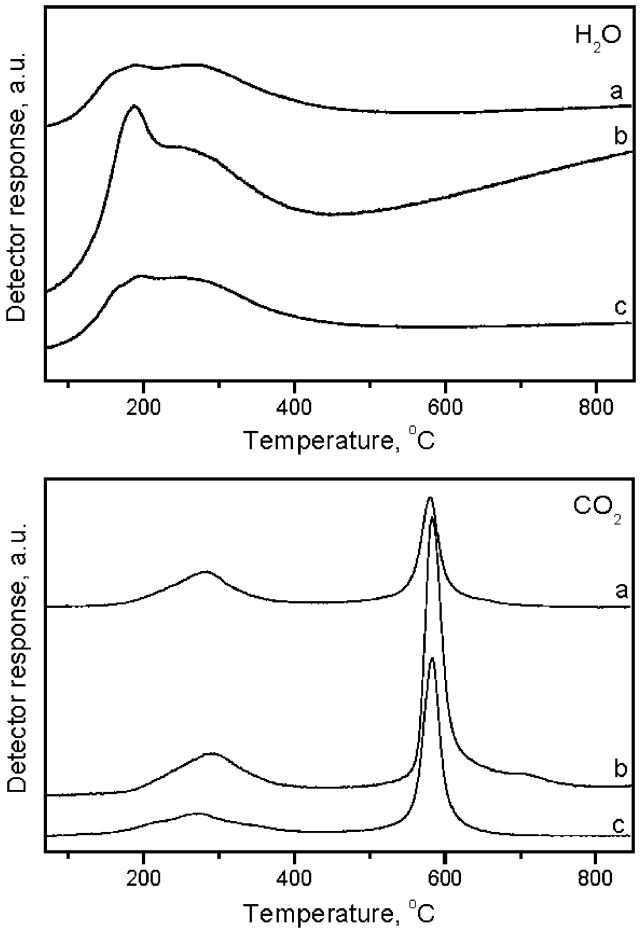

Fig. 3. MS profiles of evolved gases in situ during decomposition of (a) CuNiAl-HT, (b) CuMgAl-HT, (c) CuCoAl-HT under nitrogen.

materials irrespective of the nature of the bivalent metal ion. This observation is consistent with the above inference that the two respective thermal effects are characterizing the copper-containing phase irrespective of the co-bivalent and trivalent metal ion.

The TG and DTG curves recorded in oxygen, where oxidation processes are expected, are plotted in Fig. 4. A careful examination of these curves, and their comparison with those recorded in nitrogen (Fig. 2), shows that

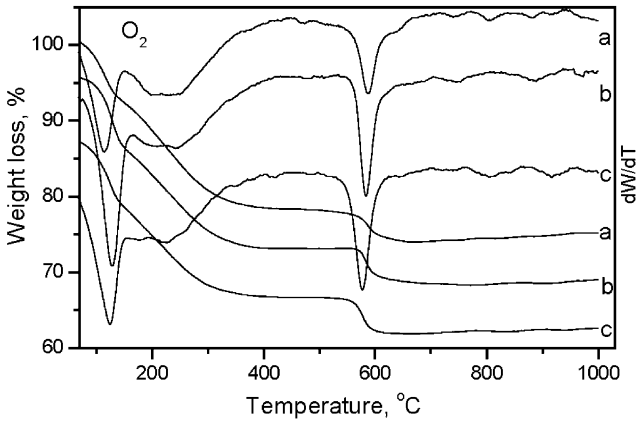

Fig. 4. TG and DTG traces of (a) CuNiAl-HT, (b) CuMgAl-HT, (c) CuCoAl-HT recorded in oxygen.

the TG curves are almost coincident below ca. 550–600°C, the main difference being the weight loss above 800°C recorded in nitrogen, but absent in oxygen. The DTG curves provide a clearer description of the differences between the processes taking place in an inert or an oxidizing atmosphere. The first sharp DTG peak corresponding to the first weight loss, is coincident for all samples when recorded in nitrogen or oxygen, thus confirming that it corresponds to non-oxidizing processes, i.e., dehydration via removal of the interlayer water molecules. However, the second process, which is recorded as a single or split process in the DTG analysis and which has been ascribed to dehydroxylation and simultaneous decarbonation, shows some differences: while it is relatively sharp or splits into two peaks in nitrogen, it is broad and ill-defined in oxygen. Such a difference as observed for sample CuCoAl-HT could possibly be attributed to the simultaneous oxidation of Co^{2+} species [21–23]. It is also known that variations in the dehydroxylation process occur with the variation in heating atmosphere and is also influenced by the nature, the oxidation state and coordination of metal ions present in the layered lattice. Further, a comparison of TG traces of CuCoAl-HT recorded in either nitrogen or oxygen shows that the curves are nearly coincident from room temperature to 200°C and between 650° and 800°C. A small difference between the curves in the range 200–650°C was noted (not observed for the other samples) with the weight loss being slightly larger when the sample was heated in nitrogen rather than in oxygen. This might indicate evidence for the oxidation of Co^{2+} to Co^{3+} in oxidizing atmosphere. Assuming the weight loss difference between the formation of 3 CoO and Co_3O_4 and considering the weight percent of cobalt present in the sample, a theoretical value of 0.63% was calculated while experimentally the value was found to be 0.9%, not too far from the theoretical value, but rather within the experimental error. Further, our earlier TPR experiments [24] demonstrated that H_2 consumption values for the calcined samples were higher than one (M/H_2 mole ratio) and the values were nearly 1.1 when considering the average oxidation state values between 2.67 and 3.0, indicating the presence of Co^{3+}. The thermal effects recorded between 400° and 600°C as well as the changes responsible for the weight loss recorded above 800°C in nitrogen are clearly related to transformations involving copper-containing species. In our earlier work, we have proposed a catalytic role of the cobivalent metal ion, namely cobalt, since a shift of the third transformation to lower temperature occurred with an increase in the concentration of cobalt. We now propose a different explanation, namely a correlation of temperature shift with variation in the copper content of the sample. The DTA curves recorded in nitrogen or in oxygen (not shown) also provided information complementing that from the TG/DTG analysis; the positions of the DTA minima approximately correspond to the positions of the minima in the DTG curves. In the low-temperature region, the DTA curves are rather similar to the DTG curves. The curves recorded in nitrogen and in oxygen are acceptably similar, with two main differences: (i) the high temperature effect is only recorded for the Cu-rich samples in nitrogen in agreement with the TG results, and (ii) the second endothermic effect is sharper in oxygen than in nitrogen, i.e., they occur in a narrower temperature range. In order to understand the nature of the phase evolution upon calcination, powder X-ray diffraction and infrared spectroscopy of these samples were carried out under in situ conditions with increasing temperatures.

Interesting information emerged upon investigating the phase evolution of these materials under in situ conditions. PXRD spectra of a representative sample CuMgAl-HT after calcination at various temperatures in air are given in Fig. 5 (diffractograms of other samples namely CuCoAl-HT and CuNiAl-HT are

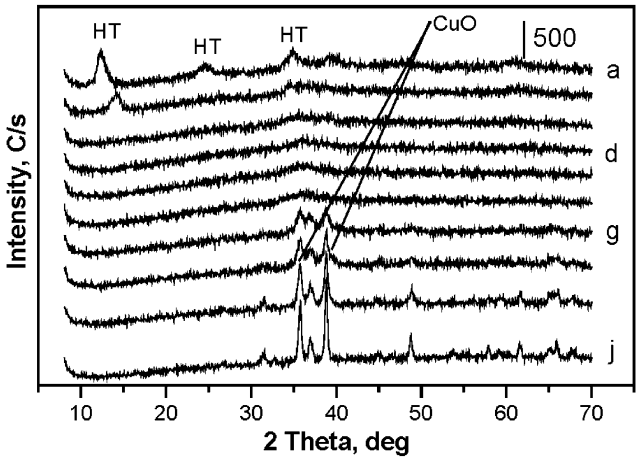

Fig. 5. PXRD patterns of CuMgAl-HT in situ calcined at (a) 50°C, (b) 100°C, (c) 150°C, (d) 200°C, (e) 300°C, (f) 400°C, (g) 500°C, (h) 600°C, (i) 700°C, (j) 800°C.

shown in Fig. 6 and 7). As reported earlier, for these materials [25], the basal reflections (003) and (006) progressively shift with increasing temperatures. This could be attributed to the removal of interlayer water accompanied by a reduction of the interlayer spacing. A closer inspection of the (003) reflection for these samples showed its complete absence at 250°C, 200°C and 150°C for CuMgAl-HT, CuNiAl-HT and CuCoAl-HT, respectively. Consequently, the stability of the layered network is highest for the Mg-containing sample followed by Ni and Co, corroborating the results obtained from thermal analysis. Interestingly, the crystallization of CuO occurs for these samples at temperatures as low as 150°C (i.e. well below the first weight loss in TG is completed). This suggests that the crystallization of CuO occurs even when the layered network prevails. This may be possible when dehydroxylation of the layered network starts at the edges of the sheets. However, the crystallinity of CuO is poor up to temperatures around 500°C. With a further increase in the temperature, the intensities of the CuO reflections (representative diffractograms are shown in Fig. 8) increase significantly. This may be correlated to the unusual third transformation seen in TG analyses, substantiating the fact, that the transformation mainly involves a copper-containing phase. With a further increase in temperature, the crystallinity of copper oxide increases, probably due to sintering. At higher temperatures, crystallization of a spinel phase, whose composition is influenced by the nature of the cobivalent metal ion, also occurs. In addition, the onset temperature of spinel crystallization varied with the nature of the cobivalent metal ion, with the crystallization being observed around 750°C for Mg- and Ni-containing systems, while it occurred already at 500°C for the Co-containing system. This clearly depicts the unusual behavior of cobalt-containing hydrotalcites [26], for which the crystallization of a spinel occurs at lower temperature, because of the facile oxidation of Co^{2+} to Co^{3+}. An attempt to identify the nature of spinels for these systems was difficult from these results, because of their poor intensities and minimal variations in the peak positions for various spinels [13, 27, 28]. It is also known that the crystallization of spinel phase increases with a further increase in calcination temperature.

In order to complement the structural transformations, infrared spectra were recorded under in situ conditions for one of the samples, namely CuMgAl-HT calcined at different temperatures under vacuum in a purpose-made cell, in which samples can be heated up to 750°C. The results are given in Fig. 9. The spectrum recorded at room temperature showed bands corresponding to synthetic hydrotalcite exhibiting broad bands in the hydroxyl region (due to extensive hydrogen bonding), a band around 1640 cm^{-1} assigned to the

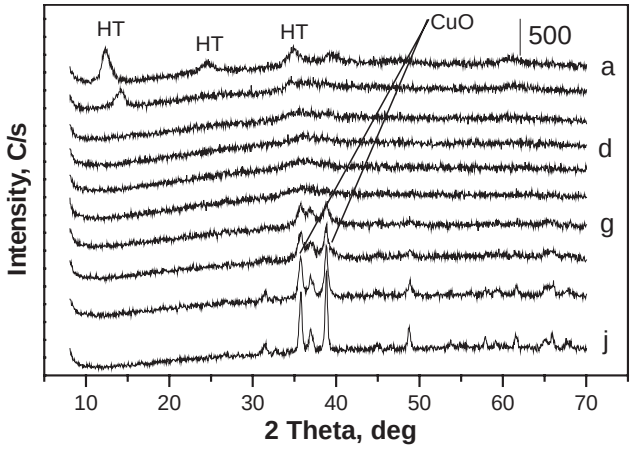

Fig. 6. PXRD patterns of CuCoAl-HT in situ calcined at (a) 50°C, (b) 100°C, (c) 150°C, (d) 200°C, (e) 300°C, (f) 400°C, (g) 500°C, (h) 600°C, (i) 700°C, (j) 800°C.

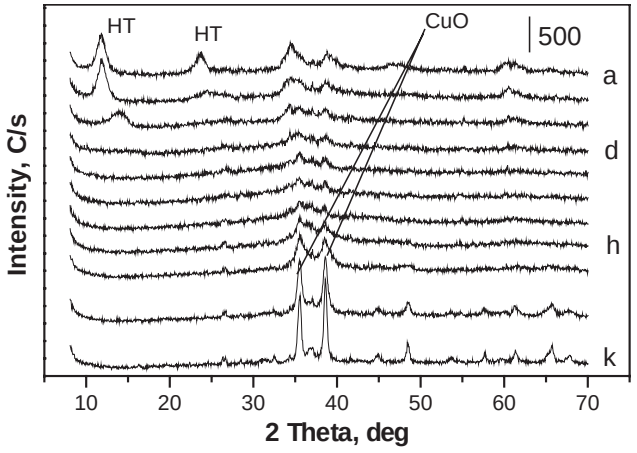

Fig. 7. PXRD patterns of CuNiAl-HT in situ calcined at (a) 50°C, (b) 100°C, (c) 150°C, (d) 200°C, (e) 300°C, (f) 400°C, (g) 500°C, (h) 600°C, (i) 700°C, (j) 800°C, (k) 850°C.

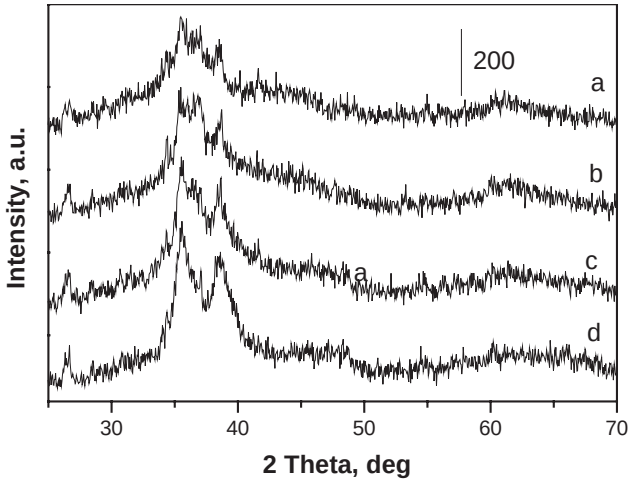

Fig. 8. PXRD diagrams of CuNiAl-HT calcined at (a) 500°C, (b) 550°C, (c) 600°C, (d) 650°C.

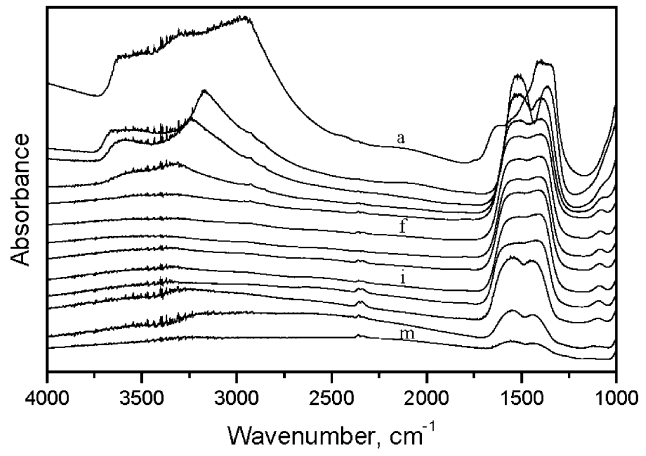

Fig. 9. In situ FT-IR spectra of CuMgAl-HT calcined at different temperatures for 30 min (a) 30°C, (b) 100°C, (c) 200°C, (d) 250°C, (e) 300°C, (f) 350°C, (g) 400°C, (h) 450°C, (i) 500°C, (j) 600°C, (k) 650°C, (l) 700°C, (m) 750°C.

deformation mode of water molecules present in the interlayer and a sharp band around 1380 cm^{-1}, assigned to the ν_3 asymmetric stretching vibration of carbonate. However, a significant change in the ν_3 vibration of carbonate was noted when the sample was calcined at 100°C. The band then splits into two well-defined bands located around 1514 and 1360 cm^{-1}. This may suggest a rearrangement of the carbonate anions in the interlayer space, caused by a partial removal of interlayer and/or physisorbed water molecules from the HT-like network. In other words, the coordination of carbonates changes upon removal of water molecules where they will then coordinate to hydroxyl groups of the layered network. Fierro and coworkers [12] also reported a similar carbonate rearrangement, for which a band splitting was observed after mild calcination of a CuZnAl system. They concluded that the carbonate coordination may be either monodentate or bidentate with the band at 1370 cm^{-1} being assigned to a C–O vibration interacting with OH groups in the brucite-like network and the other band at 1530 cm^{-1} was assigned to C=O vibration. A band was also observed at relatively higher temperatures (~250°C) around 1050 cm^{-1} (Fig. 9 spectrum-d), attributed to the ν_1 vibration of carbonate, an IR active band when the symmetry of carbonate is reduced from D_{3h} to lower symmetry (such as C_{3v} or C_{2v}) [20, 29]. In addition, there is a continuous decrease in the intensity of the hydroxyl vibrations and a complete disappearance of the deformation mode of water molecules occurs because of the desorption of physisorbed water molecules with increasing calcination temperature. At 300°C, a nearly complete disappearance of the hydroxyl vibrations was noted, suggesting the absence of OH species in the calcined material. This is in accordance with TG results (Fig. 2), although the gas evolution during TG experiments (Fig. 3) showed water elimination still above 300°C (up to 350°C). This difference is presumably caused by differences in the conditions of the experiment. The IR experiment was done under dynamic vacuum while TG was done in a flow of nitrogen. Furthermore, the carbonate vibrations are present even after complete dehydroxylation (second stage of transformation) corroborating the evolved gas analysis (EGA) results. Carbonate vibrations (see spectrum m of Fig. 9) were found even after calcination of the sample at 750°C (at which EGA did not show any peaks for CO_2 evolution) suggesting the presence of strongly bonded carbonate species in the mixed metal oxide network, probably located in the lattice as oxycarbonates; nevertheless, they should be in a low concentration or be amorphous, as no indication could be obtained from the XRD diagrams. Although the process involving decarbonation of oxycarbonate during decomposition of hydrotalcites is reported earlier [9, 10], the presence of carbonate even after treatment at 750°C under dynamic vacuum for a Cu-containing hydrotalcite network, reported here for the first time, suggests the presence of oxycarbonates. We infer, that it may not be simple carbonate based on the fact, that the intensity of the carbonate vibration is too small to be present as a metal carbonate. The splitting of the ν_3 vibration, which is at 1425 cm^{-1} for the free carbonate, was found to be 158 cm^{-1}. It is possible to determine the coordination of a C_{2v} carbonate (mono- or bidentate) in the interlayer space from this splitting, which was suggested to be ca. 100 and 300 cm^{-1} for uni- and bidentate carbonates, respectively [30]. After rearrangement only one pair of bands was observed indicating that only one of the two possible coordinations depicted in Scheme 1 can be present. The experimentally observed splitting of the ν_3 carbonate vibration is indicative of a unidentate coordination of the carbonate.

The Anton Paar camera attached to our XRD for high-temperature studies has a high temperature limit of 900°C. Therefore, to investigate the phase evolution in both oxygen and nitrogen, PXRD was carried out for samples CuNiAl-HT and CuCoAl-HT after ex situ calcination at temperatures of 400, 650 and 1000°C (temperatures were chosen on the basis of TG traces). The corresponding diffraction patterns are shown in Figs. 10 and 11. The diffraction patterns observed for

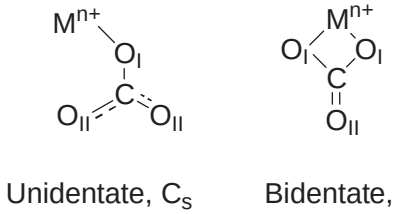

Scheme 1. Modes of co-ordination of carbonate ion with metal center.

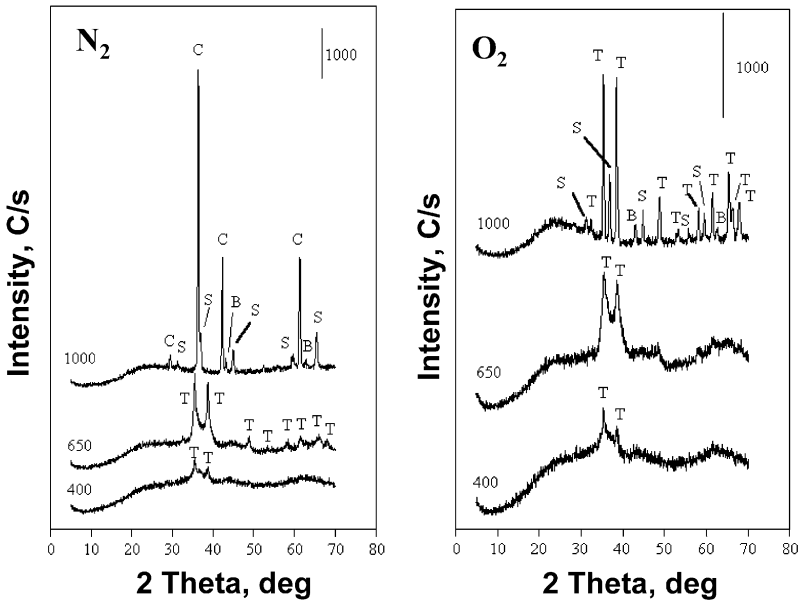

Fig. 10. PXRD diagrams of CuNiAl-HT thermally treated at designated temperatures in nitrogen and oxygen for 1 h (T—Tenorite; B—Bunsenite; S—Spinel; C—Cuprite).

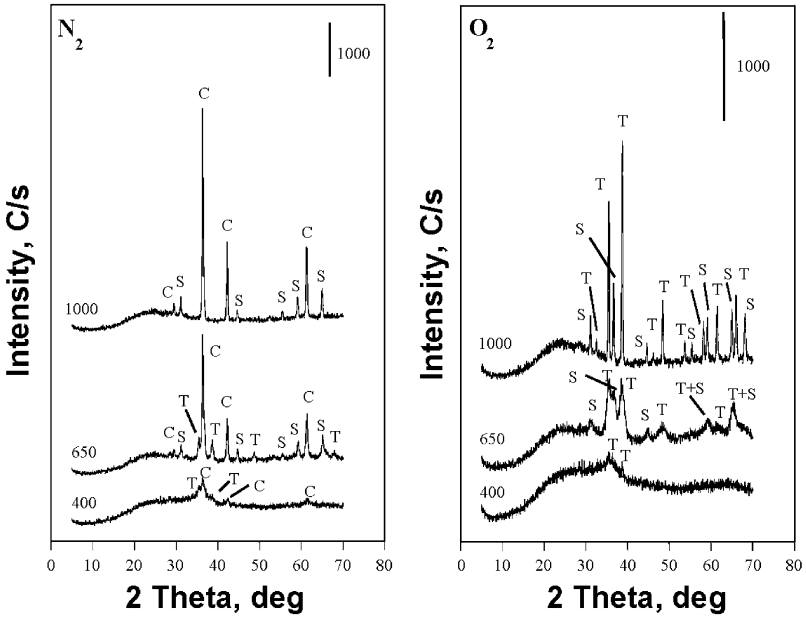

Fig. 11. PXRD diagrams of CuCoAl-HT thermally treated at designated temperatures in nitrogen and oxygen for 1 h (T—Tenorite; B—Bunsenite; S—Spinel; C—Cuprite).

samples calcined at 1000°C in either oxygen or nitrogen will clearly characterize the nature of the phases formed, as the temperature is well above all the total weight losses recorded by thermogravimetry. The phases identified are the following:

CuNiAl in nitrogen: Mainly cuprite (Cu_2O) was formed along with weak reflections of a spinel phase (which may be $CuAl_2O_4$ or $NiAl_2O_4$ or solid solutions thereof). Pure NiO (bunsenite) was also noted, however, pure tenorite (CuO) was not detected. Because of the high concentration of copper present in the sample, the formation of $CuAl_2O_4$, possibly containing small amounts of nickel, is most likely.

CuNiAl in oxygen: Main peaks correspond to tenorite with weak reflections of spinel and NiO. However, no cuprite phase was detected.

CuCoAl in nitrogen: Dominant peaks again characterize cuprite. However, additional less intense peaks characterizing a spinel were also noted. The diffraction patterns of most first row transition metal ions spinels are very similar, so that a discrimination between Cu- and Co-spinel is difficult. A peak search tentatively

suggested that $CoO \cdot Al_2O_3$, i.e. Co^{2+} spinel is the more likely structure. This is not unusual, as under non-oxidizing conditions, the oxidation of Co^{2+} to Co^{3+} is unlikely.

CuCoAl in oxygen: The main peaks correspond to tenorite like CuNiAl system, with no peaks of cuprite found. Additional spinel peaks may correspond to mixed spinels with Cu^{2+}, Co^{2+}, Co^{3+} and Al^{3+} being present.

It is known that thermodynamically favored red Cu_2O is formed by decomposition of CuO at high temperatures preferably under inert conditions [31]. We believe, that the final high-temperature transformation, which was noted in nitrogen but not in oxygen characterizes the decomposition of CuO to Cu_2O. The quantitative weight loss values can be compared with the theoretically expected values. Formation of Cu_2O from CuO can be written as

$$2CuO \rightarrow Cu_2O + 1/2O_2.$$

Hence, 2×63.54 g of copper can release 16 g of oxygen. Considering the weight percentage of copper present in CuNiAl-HT (35.8%), CuCoAl-HT (34.9%) and CuMgAl-HT (39.3%), the expected amounts of oxygen released (for 100 g of solid) are 4.5, 4.4 and 4.9 g. Experimentally, the high-temperature weight loss in nitrogen yielded 4.4, 4.6 and 4.6 g for CuNiAl-HT, CuCoAl-HT and CuMgAl-HT, respectively (Table 3). These values are sufficiently close to the theoretical values to support the interpretation of the high-temperature transformation. We emphasize that under nitrogen no copper was present as CuO as evidenced from PXRD. Hence, one can conclude that the high-temperature weight loss occurring (around 850°C) in nitrogen for these samples corresponds to quantitative formation of Cu_2O.

The samples were also treated at intermediate temperatures (i.e. after the second and third transformation in the TG traces) and studied for their phases using PXRD (also shown in Figs. 10 and 11). PXRD of CuNiAl-HT thermally treated at 400°C in nitrogen showed reflections corresponding to tenorite. The PXRD traces were nearly coincident for samples calcined either in nitrogen or in oxygen, suggesting that redox processes do not occur at 400°C. When the temperature was raised to 650°C, also only tenorite was detected, but with increased crystallinity, probably due to aggregation of the particles, which was more favored in nitrogen than in oxygen. However, when the temperature was raised to 1000°C development of Cu_2O peaks was noted in nitrogen, but not in oxygen as discussed above. These results confirm that reduction of Cu^{2+} to Cu^{+} occurs after the fourth stage of transformation (cf. quantitative TG analysis) for this sample. To confirm our results, an independent experiment was carried out wherein pure CuO (Merck) was calcined under both nitrogen and oxygen and cooled under respective atmospheres and followed both by PXRD and thermal analysis. As observed for our samples, a weight loss of around 10% was noted when CuO was calcined in nitrogen in accordance with the equilibrium $2CuO \Leftrightarrow Cu_2O + \frac{1}{2}O_2$ and PXRD (Fig. 12)

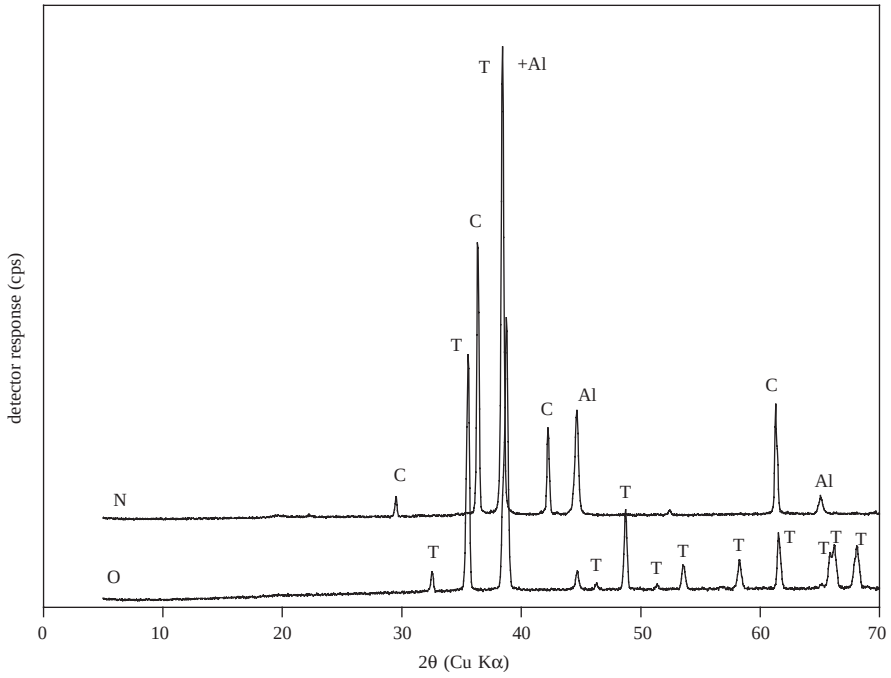

Fig. 12. PXRD diagrams of CuO calcined under nitrogen and oxygen at 1000°C for 2 h (T—Tenorite; C—Cuprite). Peaks marked Al are due to the sample holder and used as reference.

also substantiated the formation of Cu_2O, while CuO remains unchanged without any weight loss even after calcination at 1000°C when the atmosphere was oxygen.

The PXRD pattern of CuCoAl-HT thermally treated in oxygen showed peaks corresponding to tenorite at 400°C while at 650°C, peaks corresponding to a spinel phase appeared (cf. in situ PXRD results). Further increase in temperature enhanced the crystallinity of both tenorite and spinel phases. In contrast, cuprite formation along with tenorite was noticed even at 400°C when the sample was thermally treated in nitrogen. At 650°C, the crystallinity of both phases was improved and a spinel phase was formed. Thermal treatment at 1000°C did not yield peaks corresponding to tenorite but only cuprite and a spinel phase were detected. The formation of the cuprite phase at lower temperatures may be caused by a catalytic role played by cobalt in reducing Cu^{2+} to Cu^{+}. The formation of Cu_2O at lower temperatures poses a doubt on the quantification of the fourth stage of transformation for this sample. However, we believe, the concentration of such species is less

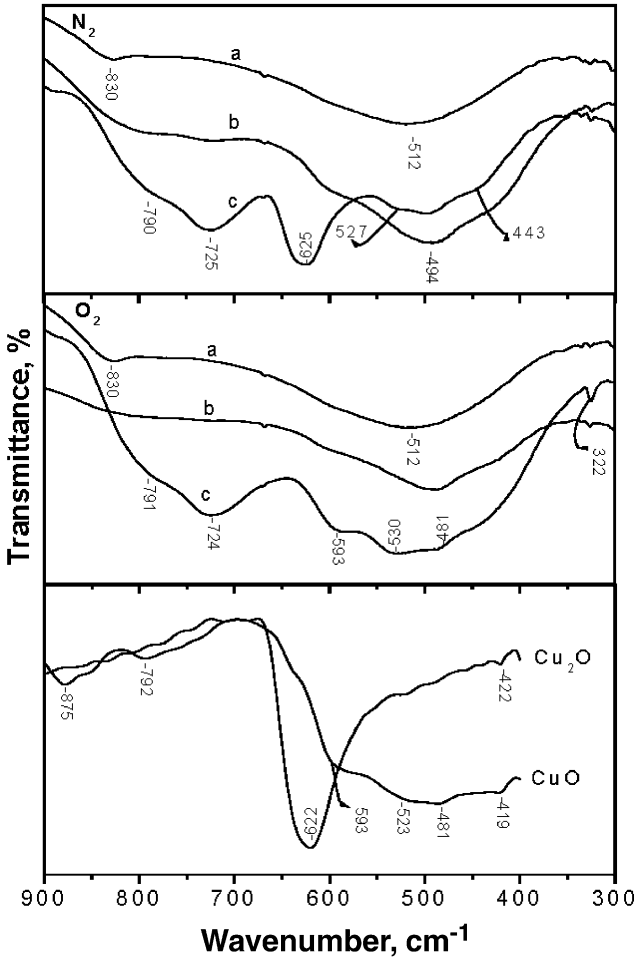

Fig. 13. FT-IR spectra of CuNiAl-HT thermally treated at (a) 400°C, (b) 650°C, and (c) 1000°C in nitrogen and oxygen; spectra of Cu_2O and CuO are included for comparison.

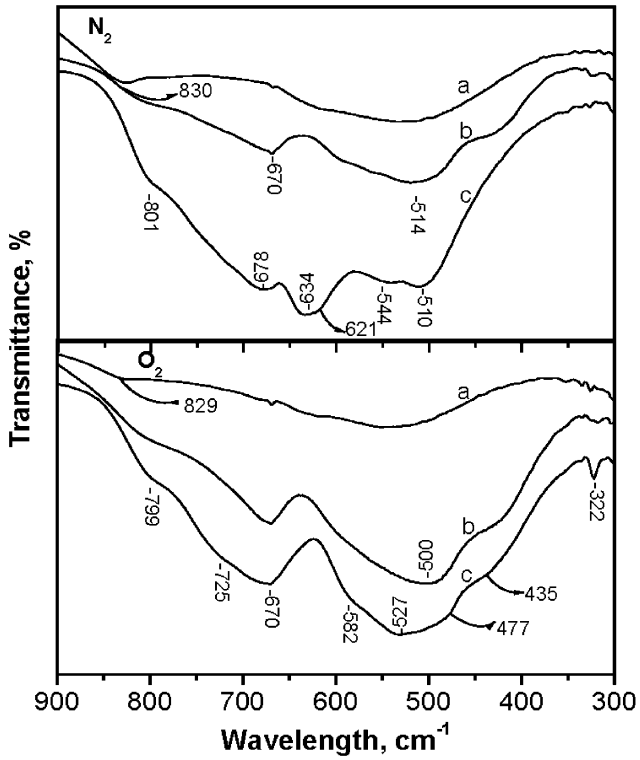

Fig. 14. FT-IR spectra of CuCoAl-HT thermally treated at (a) 400°C, (b) 650°C, and (c) 1000°C in nitrogen and oxygen.

(although it is well crystalline in nature) at lower temperatures while it increases with an increase in thermal treatment temperature (at the expense of the concentration of CuO). However, one cannot completely exclude the contribution of the thermodynamically allowed decomposition of Co_3O_4 to CoO under nitrogen at around this temperature (850°C) during the fourth stage of transformation [32].

In order to elucidate further on these findings, FT-IR spectra of the calcined samples were recorded at various temperatures (similar to PXRD) and are reported in Figs. 13 and 14. The spectra of authentic samples, namely Cu_2O and CuO, are also presented for comparison in Fig. 13.

The spectrum of the CuNiAl sample thermally treated in nitrogen at 400°C does not exhibit well-defined bands except for a weak band around 830 cm^{-1}, which is assigned to the out-of-plane deformation mode (ν_2) of carbonate [33]. A broad absorption band around 512 cm^{-1} was observed, which could not give any relevant information. The spectrum recorded in oxygen was identical to that observed in nitrogen consistent with PXRD results, which suggested that no redox transformation occurs at this temperature. However, when the sample was thermally treated at 650°C in either nitrogen or oxygen, no band was noted at 830 cm^{-1} which suggests the absence of carbonate or that the carbonate is present in undetectably low

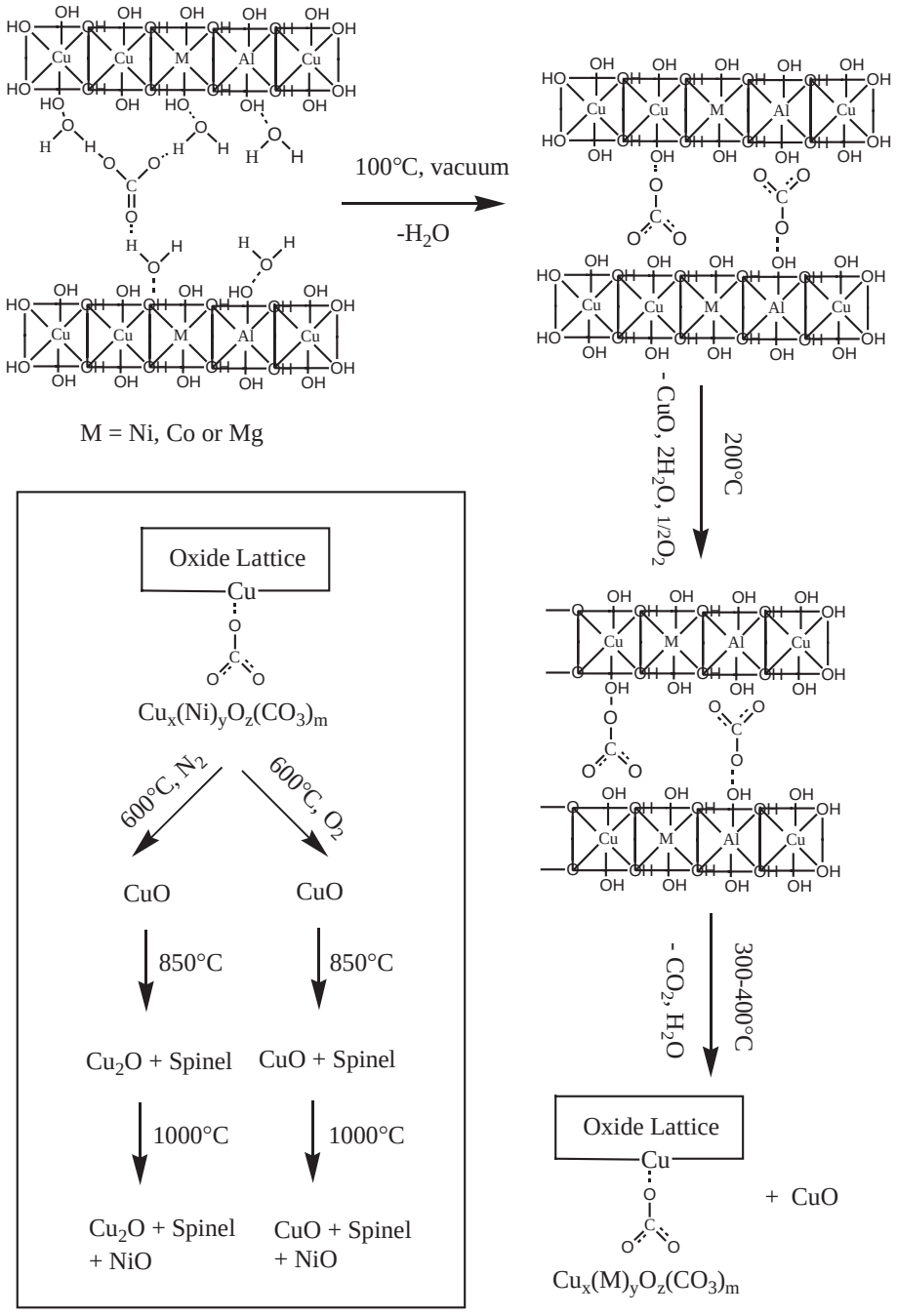

Scheme 2. Thermal evolution processes involved in heating of Cu-rich hydrotalcites.

concentration. The spectral vibrations due to *M*–O vibrations were better resolved and absorptions were noted around 494 cm^{-1} (ν_1, ν_{Cu-O}) and around 600 cm^{-1} confirming the presence of CuO [34]. In addition, very weak bands around 730 and 800 cm^{-1} (including a broad absorption around 600 cm^{-1}) were noted, probably assigned to absorptions of spinel, although PXRD did not reveal a crystalline spinel phase at this temperature [35], suggesting that they are either amorphous or poorly crystallized. No well-defined absorption was noted for the sample calcined in oxygen, again corroborating PXRD results, which showed poor crystallinity of tenorite formed in oxygen in contrast to nitrogen. The spectra recorded both in oxygen and nitrogen showed clear features when the sample was thermally treated at 1000°C. In the case of nitrogen, a sharp band characteristic of cuprite was noted around 625 cm^{-1} (see Fig. 13). No bands were noted in the region around 500 and 600 cm^{-1}, characteristic of tenorite, as supported by PXRD (Fig. 10). The bands due to the spinel phase also sharpened with clear features around 725 cm^{-1} (ν_1 vibration of spinel

phase) and 790 cm^{-1}. Although we do not have an evidence to prove the band around 800 cm^{-1} is for the spinel phase, we do observe such a weak band around 800 cm^{-1} for pure binary CoAl hydrotalcite calcined at 400°C in air for 5 h and for pure Co_3O_4 [21]. However, bands characteristic of tenorite were detected in oxygen (bands at 593, 530 and 480 cm^{-1}) along with bands of the spinel phase. The band positions of the spinel phase were similar irrespective of the atmosphere, suggesting a similar nature of the spinel phase in both cases.

Subtle differences were noted for sample CuCoAl-HT when the thermal treatment was carried out in different atmospheres. FT-IR spectra (Fig. 14) of the sample treated both in nitrogen and oxygen at 400°C, showed a broad absorption from which no discrete information could be inferred. However, similar to CuNiAl-HT, the ν_2 absorption of carbonate was also observed for this system. When the treatment temperature was raised to 650°C, a sharp band around 670 cm^{-1} was noted, ascribed to a spinel vibration [35]. A broad band was noted in the region 650–500 cm^{-1} with weak bands around 600 and 560 cm^{-1}, although PXRD showed well-crystallized Cu_2O peaks for this sample. In other words, although PXRD showed the formation of cuprite, FT-IR did not clearly reveal its formation (band around 635 cm^{-1} might be buried in the broad band between 650 and 550 cm^{-1}), suggesting that the concentration of this phase must be very low, however, highly crystalline. However, when the sample was thermally treated at 1000°C in nitrogen, a well-defined band characteristic of cuprite was noted at 634 cm^{-1} and no band due to tenorite was detected. Further, a shift in the band position for the spinel phase occurs, probably due to compositional variations, due to incipient crystallization of the cuprite phase. Bands (585, 525 and 480 cm^{-1}) corresponding to tenorite were noted in oxygen for the sample calcined at 1000°C. However, in oxygen, no significant shift in the band position was seen for the spinel phase, whose intensity was much larger than for the spinel phase observed in nitrogen (similar to PXRD results; see Fig. 11). Further, the bands due to spinel are relatively broad, suggesting the presence of multivalent metal ions (in other words, occurrence of oxidation) present both in tetrahedral and octahedral coordination. Weak shoulders were also noted for the sample calcined in oxygen around 725 and 800 cm^{-1} substantiating the presence of the spinel phase. In addition, both samples showed a sharp band around 320 cm^{-1} when calcined in oxygen at 1000°C, for which the attribution is not clear.

5. Conclusions

Single-phase Cu*M*(II)Al ternary hydrotalcites with (Cu + *M*(II))/Al atomic ratio 3.0 and Cu/*M*(II) atomic ratio around 5.0 were synthesized. The thermal analysis pattern of these samples showed four weight loss stages in nitrogen with the fourth stage being ascribed to reduction of CuO to Cu_2O (not observed when recorded in oxygen). Formation of CuO (by in situ PXRD) through partial dehydroxylation of the layered network was noted well below the structural decomposition. Retention of carbonate at temperatures as high as 700°C (in situ FT-IR) was noted suggesting the presence of oxycarbonate. Based on the discussions presented above, thermal evolution processes involved on heating Cu-rich hydrotalcites in both inert and oxidizing atmospheres are given in Scheme 2.

Acknowledgments

S.K. thanks the Alexander von Humboldt Foundation for a research fellowship. S.K. also thanks the Council of Scientific and Industrial Research, New Delhi, for financial assistance under Young Scientist Scheme. V.R. thanks MCyT (Spain) for Grant MAT2000-1148-C02-01.

References

[1] F. Trifirò, A. Vaccari, in: J.L. Atwood, J.E.D. Dasvies, D.D. MacNicol, F. Vogtle, J-M. Lehn, G. Alberti, T. Bein (Eds.), Comprehensive Supramolecular Chemistry, Solid State Supramolecular Chemistry: Two and Three-dimensional Inorganic Networks, Vol. 7, Pergamon, Oxford, 1996, pp. 251–291.
[2] V. Rives (Ed.), Layered Double Hydroxides: Present and Future, Nova Sci. Pub. Inc., New York, 2001.
[3] J.G. Nunan, P.B. Himelfarb, R.G. Herman, K. Klier, C.E. Bogdan, G.W. Simmons, Inorg. Chem. 28 (1989) 3868–3874.
[4] M. Trombetta, G. Ramis, G. Busca, B. Montanari, A. Vaccari, Langmuir 13 (1997) 4628–4637.
[5] A. Corma, A.E. Palomares, F. Rey, F. Márquez, J. Catal. 170 (1997) 140–148.
[6] A. Dubey, V. Rives, S. Kannan, J. Mol. Catal. A 181 (2002) 151–160.
[7] A. Dubey, S. Kannan, S. Velu, K. Suzuki, Appl. Catal. A 238 (2003) 319–326.
[8] G.L. Castiglioni, G. Minelli, P. Porta, A. Vaccari, J. Solid State Chem. 152 (2000) 526–532.
[9] V. Rives, S. Kannan, J. Mater. Chem. 10 (2000) 489–495.
[10] S. Velu, C.S. Swamy, J. Mater. Sci. Lett. 15 (1996) 1674–1677.
[11] A. Alejandre, F. Medina, P. Salagre, X. Corregi, J.E. Sueiras, Chem. Mater. 11 (1999) 939–948.
[12] I. Melian-Caberera, M. Lopez Granados, J.L.G. Fierro, Phys. Chem. Chem. Phys. 4 (2002) 3122–3127.
[13] Joint Committee on Powder Diffraction Standards (Set No. 46), International Centre for Diffraction Data, Pennsylvania, 1996
[14] V. Rives, Ads. Sci. Technol. 8 (1991) 95–104.
[15] A. De Roy, C. Forano, K. El Malki, J.P. Besse, in: M.L. Occelli, H. Robson (Eds.), Expanded Clays and Other Microporous Solids, Synthesis of Microporous Materials, van Nostrand Reinhold, New York, 1992, pp. 108–126 (Chapter 7).
[16] S. Kannan, Appl. Clay Sci. 13 (1998) 347–362.
[17] M.J.L. Gines, C.R. Apesteguia, J. Therm. Anal. 50 (1997) 745–756.

[18] Y. Lwin, M.A. Yarmo, Z. Yaakob, A.B. Mohamad, W.R.W. Daud, Mater. Res. Bull. 36 (2001) 193–198.
[19] R.D. Shannon, C.T. Mitchell, Acta Crystallogr. B 25 (1969) 925–945.
[20] S. Kannan, S. Velu, V. Ramkumar, C.S. Swamy, J. Mater. Sci. 30 (1995) 1462–1468.
[21] S. Kannan, C.S. Swamy, J. Mater. Sci. 32 (1997) 1623–1630.
[22] R. Xu, H.C. Zeng, Chem. Mater. 13 (2001) 297–303.
[23] L. Chmielarz, P. Kustrowski, A. Rafalska-Lasocha, D. Majda, R. Dziembaj, Appl. Catal. B 35 (2002) 195–210.
[24] V. Rives, A. Dubey, S. Kannan, Phys. Chem. Chem. Phys. 3 (2001) 4826–4836.
[25] E. Kanezaki, Inorg. Chem. 37 (1998) 2588–2590.
[26] F. Kooli, V. Rives, M.A. Ulibarri, Inorg. Chem. 34 (1995) 5122–5128.
[27] U. Chellam, Z.P. Xu, H.C. Zeng, Chem. Mater. 12 (2000) 650–658.
[28] H.C. Zeng, Z.P. Xu, M. Qian, Chem. Mater. 10 (1998) 2277–2283.
[29] V. Rives, Mater. Chem. Phys. 75 (2002) 19–25.
[30] G. Busca, V. Lorenzelli, Mater. Chem. 7 (1982) 89–126.
[31] F.A. Cotton, G. Wilkinson, C.A. Murillo, M. Bochmann, Advanced Inorganic Chemistry, 6th Edition, John Wiley and Sons, Inc., New York, 1999, p. 856.
[32] Z.P. Xu, H.C. Zeng, J. Mater. Chem. 8 (1998) 2499–2506.
[33] J. Perez-Ramirez, G. Mul, J.A. Moulijn, Vib. Spectrosc. 27 (2001) 75–88.
[34] J.A. Goldsmith, S.D. Ross, Spectrochim. Acta 24A (1968) 2131–2137.
[35] J. Preudhomme, P. Tarte, Spectrochim. Acta 27A (1971) 1817–1835.